

Accepted Manuscript

Study of the effects of ionic liquid-modified cathodes and ceramic separators on MFC performance

V.M. Ortiz-Martínez, I. Gajda, M.J. Salar-García, J. Greenman, F.J. Hernández-Fernández, I. Ieropoulos

PII: S1385-8947(16)30052-3
DOI: <http://dx.doi.org/10.1016/j.cej.2016.01.084>
Reference: CEJ 14703

To appear in: *Chemical Engineering Journal*

Received Date: 22 October 2015
Revised Date: 19 January 2016
Accepted Date: 22 January 2016

Please cite this article as: V.M. Ortiz-Martínez, I. Gajda, M.J. Salar-García, J. Greenman, F.J. Hernández-Fernández, I. Ieropoulos, Study of the effects of ionic liquid-modified cathodes and ceramic separators on MFC performance, *Chemical Engineering Journal* (2016), doi: <http://dx.doi.org/10.1016/j.cej.2016.01.084>

This is a PDF file of an unedited manuscript that has been accepted for publication. As a service to our customers we are providing this early version of the manuscript. The manuscript will undergo copyediting, typesetting, and review of the resulting proof before it is published in its final form. Please note that during the production process errors may be discovered which could affect the content, and all legal disclaimers that apply to the journal pertain.



1 **Study of the effects of ionic liquid-modified**
2 **cathodes and ceramic separators on MFC**
3 **performance**

4 V.M. Ortiz-Martínez^{1,*}, I. Gajda², M.J. Salar-García¹, J. Greenman², F.J.
5 Hernández-Fernández¹, I. Ieropoulos^{2,*}.

6
7 (1) Polytechnic University of Cartagena, Chemical and Environment Engineering
8 Department, Campus Muralla del Mar, C/Doctor Fleming S/N, E-30202 Cartagena,
9 Murcia.

10
11 (2) Bristol BioEnergy Centre, Bristol Robotics Laboratory, Block T, UWE, Bristol,
12 Coldharbour Lane, Bristol BS16 1QY, UK.

13
14 *Corresponding author. E-mail address: ioannis.ieropoulos@brl.ac.uk; victor.ortiz@upct.es

15
16 **ABSTRACT**

17 Ceramic-based MFC designs have proven to be a low cost alternative for power
18 production and wastewater treatment. The use of ionic liquids in ceramic MFCs
19 is explored for the first time in the present work in order to improve power
20 output. The ionic liquid (IL) 1-ethyl-3-methylimidazolium
21 bis(trifluoromethylsulfonyl)imide, [EMIM][Tf₂N], has been selected for this
22 purpose due to its advantageous properties. The performance of activated
23 carbon cathodes using polytetrafluoroethylene (PTFE) binder and different
24 carbon diffusion layers (DL) (controls) are compared with two types of ionic

25 liquid-modified cathodes (test). This work continues to study the performance of
26 terracotta separators modified with the same ionic liquid, neat and also mixed
27 with PTFE. While the results show operational limitations when the IL is
28 integrated in the ceramic separator, there is a significant enhancement of the
29 MFC performance when added as part of the activated layer mixture of the
30 cathode, achieving up to 86.5 % more power output in comparison with IL-free
31 MFCs (from 229.78 μW to 428.65 μW). The addition of a layer of PTFE-mixed
32 ionic liquid spread on the activated layer of the cathode also leads to an
33 increase in power of approximately 37 %.

34

35 **Keywords: Ceramic separators; Microbial Fuel Cell; Ionic liquid; Activated**
36 **carbon cathodes; Activated sludge.**

37

38 **1. Introduction.**

39 Microbial Fuel Cells (MFCs) have been extensively investigated in recent years
40 since this technology offers promising prospects for bioenergy production from
41 wastewater. In the context of the current global energy crisis and growing
42 demands for water treatment, the scientific community sees the development of
43 this technology as a potential alternative that may help address such pressing
44 issues [1, 2]. Although the performance of this technology has increased almost
45 exponentially in the last two decades, there are some limitations associated with
46 the low levels of power density achieved and their operating and fabrication
47 costs [3]. Thus, the improvement of efficiency in MFC performance requires the
48 study of non-expensive materials and simpler designs [4, 5].

49 The great potential of MFC technology lies in the direct conversion of the
50 chemical energy stored in organic wastes and biomass into electricity, operating
51 at ambient conditions without additional energy requirements and with a net
52 balance of zero emissions [6]. In the process, electrons are released and
53 transported to the cathode through an external circuit while obtaining an
54 electrical current. In double and single-chamber MFCs the use of a membrane
55 or separator allows the ion exchange mechanism to take place while
56 maintaining the anode and cathode chambers physically separated [7]. The
57 selection of the appropriate separator is one of the key factors in designing
58 MFC devices. The high cost of proton exchange membranes based on
59 perfluored polymers such as Nafion reduces the efficiency of this technology
60 and, therefore, a wide range of separator materials have been investigated in
61 the last years, including cation and anion exchange membranes, glass fibers or
62 porous fabrics, among other alternatives [8]. Paper in combination with
63 conductive latex and microporous polymer-based carbon are other examples of
64 alternative separators made out of porous material being currently developed
65 [9,10]. Ceramic-based separators have proven to be a low cost alternative in
66 MFCs. Park *et al.* [11] used a porcelain-coated cathode as proton exchange
67 layer replacing expensive proton-selective membranes. Most recently, earthen
68 pot and terracotta have been evaluated as separators in MFCs showing their
69 capacity for proton transfer and power production [12, 13], reaching sufficient
70 power for practical applications in the absence of metal catalysts [14]. The use
71 of ceramic and precious metal-free MFCs has effected major cost reductions in
72 this technology. The thickness of the ceramic wall or the porosity are important
73 factors that affect the cell performance [13]. The electrode material is another

74 key factor directly affecting the performance of MFCs and their feasibility from
75 both an economic and long-term operation point of view [15]. Several types of
76 carbon-based materials such as carbon nanofibers (CNF), carbon nanotubes
77 (CNT) or activated carbon (AC) have been researched as electrode materials,
78 showing high surface area and catalytic activity for an effective oxygen
79 reduction reaction at the cathode [16-19]. Amongst them, activated carbon
80 offers competitive advantages such as low cost and high catalytic activity [14,
81 20].

82 The present work explores the enhancement of the power performance of
83 ceramic MFCs employing metal-free activated-carbon based electrodes through
84 the incorporation of ionic liquids as part of the cathode. It has been reported that
85 the potential of the cathode in ceramic-based MFCs can limit the power
86 production, thus demanding more emphasis for the improvement of the cathode
87 performance [12]. Because of the distinctive properties of ionic liquids, the
88 range of applications of this type of compounds has widened greatly in recent
89 years, including separation processes, chemical catalysis or biological systems
90 [21]. A typical IL is based on the combination of organic cations (e.g. N-
91 alkylpyridinium, N,N'-dialkylimidazolium) and a mono- or poly-atomic inorganic
92 anion (e.g. e.g. Cl^- , AlCl_4^- , PF_6^-) or, increasingly more common, an organic
93 anion (e.g. $(\text{CF}_3\text{SO}_2)_2\text{N}^- = \text{Tf}_2\text{N}^-$, $(\text{C}_2\text{F}_5\text{SO}_2)_2\text{N}^- = \text{Pf}_2\text{N}^-$) [22]. Their
94 environment-friendly characteristics, thermal stability, high ionic conductivity
95 and wide electrochemical window ($\approx 4\text{-}6\text{ V}$) make them suitable candidates for
96 several electrochemical systems [23], having been employed in batteries and
97 capacitors, solid-state electrochemical actuators, electrochemical sensors and
98 fuel cells [22]. Several groups have also studied the performance of ionic liquids

99 as electrolytes in proton exchange membrane fuel cells (PEMFCs), including
100 MFCs [24-26]. The terracotta material itself has been used as an ion exchange
101 separator and MFC chassis. Some limitations have been posed by this type of
102 material, such as possible oxygen diffusion through the porous wall into the
103 anode chamber [12]. The present work also investigates the possibility of using
104 the ionic liquid as an electrolyte by directly applying it onto the ceramic
105 separator. Ionic liquids have been used as electrolytes in a wide range of
106 electrochemical processes and devices due to their good properties, being
107 characterised by negligible vapour pressure [27, 28]. These advantages have
108 made possible the replacement of conventional electrolytes with ionic liquids,
109 avoiding volatility and chemical stability problems [29]. In the present study, 1-
110 ethyl-3-methylimidazolium bis(trifluoromethylsulfonyl)imide, [EMIM][Tf₂N], has
111 been selected to assess the use of ILs for improving the power performance in
112 ceramic MFCs for the first time. This imidazolium-based IL was chosen due to
113 its advantageous properties such relatively high ionic conductivity compared
114 with the typical conductivity range for other ionic liquids (9 mS.cm⁻¹ at RT [29]),
115 good chemical stability, low viscosity (37 cp at RT) and hydrophobic nature [28]
116 . The influence of the IL selected on the MFC performance is studied in terms of
117 power generation when added as part of the cathode and on the separator
118 (ceramic wall).

119

120 **2. Materials and methods.**

121 **2.1. MFC configuration and operation.**

122 Fig.1 shows a schematic representation of the Microbial Fuel Cells used in this
123 study. The units were set up with terracotta bottom sealed cylinders (Weston
124 Mill Pottery, Nottinghamshire, UK) of 10 cm length, with 3.5 cm and 4 cm, inner
125 and outer diameter, respectively, and wall thickness of 3 mm. The terracotta
126 material used is characterized by a water absorption amount (by weight) of 9.1
127 % (SD 0.4) [30]. The cylinders were placed in bottle-shaped plastic housing
128 covered on top with a layer of Parafilm®, which forms the anode compartment,
129 with a maximum fuel capacity of 160 ml. The anode electrode was a layer of
130 carbon fibre veil (loading 20 g.m⁻²) in a rectangular shape with a total macro
131 surface area of 2430 cm² (PRF Composite Materials, Dorset, UK), folded and
132 wrapped around the outside of the terracotta caves and held with nickel-
133 chromium wire; the latter also served as the current collector and connection
134 point. MFCs were fed with full strength or 1:10 diluted activated sewage sludge
135 (Wessex Water Scientific Laboratory, Cam Valley, Saltford, UK) in distilled
136 water and supplemented with sodium acetate anhydrous (Fisher chemical,
137 Loughborough, UK) to ensure sufficient carbon energy for the microorganisms
138 during the operation of the MFCs. Two conditions of substrate concentration (20
139 and 100 mM) were employed in order to study the effects of substrate
140 concentration on power performance and, in turn, compare this with that of the
141 ionic liquid. The MFCs employed were operated in batch mode and loaded with
142 an external resistance of 100 Ω. The anode of each MFC was matured for two
143 weeks, prior to starting the experiments, by periodically feeding the anode with
144 a solution of sludge and acetate (100 mM).

145

[INSERT FIGURE 1]146 **2.2. Preparation of the cathodes and the ceramic separators.**

147 Several activated carbon-based cathodes were fabricated and their
148 performance was compared in terms of power production. The general way to
149 prepare the cathodes involves hot pressing a mixture of 80 g of activated
150 carbon (AC) powder (G. Baldwin and Co., London, UK) and 20 wt% of
151 polytetrafluoroethylene (PTFE) in 120 ml of deionized water, onto the diffusion
152 layer (carbon veil or carbon cloth), which was previously coated with PTFE (60
153 % PTFE dispersion in water, Sigma Aldrich, UK), as described in [14]. The final
154 dimensions of the cathodes were 9x10 cm and the final loading of activated
155 carbon was approximately 60 mg.cm⁻² per cathode. Once the AC mixture is dry,
156 the cathodes are placed inside the terracotta cylinders (cathode compartment),
157 with the side of the AC loading in contact with the inner wall of the ceramic
158 cylinder and the diffusion layer exposed to air. As a preliminary study, the
159 behaviour of two types of carbon materials were tested as substratum/diffusion
160 layers namely, carbon veil (cathode-1) (20 g.m⁻², air permeability 420
161 cm³/cm²/sec, PRF Composite Materials, Dorset, UK) and carbon cloth (cathode-
162 2) (120 g.m⁻², air permeability 100 cm³/cm²/sec, 100% activated, Zorflex[®],
163 Feluy, Belgium).

164 The performance of the ionic liquid 1-ethyl-3-methylimidazolium
165 bis(trifluoromethylsulfonyl)imide [EMIM][Tf₂N] (Ionic Liquids Technologies,
166 Heilbronn, Germany), was first investigated in the ceramic MFCs as part of the
167 cathode. Two cathode structures were fabricated for this purpose. The first
168 modified type was prepared by mixing AC, PTFE and deionised water as
169 described above and hot pressing the mixture onto carbon veil. Once the
170 cathode is dry, a layer of ionic liquid mixed with PTFE (60 % dispersion in
171 water) is applied uniformly over the side of the AC mixture (cathode-3). The

172 second modified type of AC-based cathode was prepared by mixing AC, PTFE,
173 deionised water and the ionic liquid under study at the same time, and then hot
174 pressing the final mixture onto carbon veil until the cathode is dry (cathode-4).

175 The fabrication of the cathodes was manual and thus it is difficult to provide an
176 accurate thickness, which ranged between 1.5-2 mm, at a fixed carbon loading
177 of 60 mg.cm^{-2} for all cathodes prepared.

178 The inner wall of the terracotta cylinders, which acts as separator between the
179 cathode and the anode chamber of the MFCs set up [31], was modified with
180 $[\text{EMIM}][\text{Tf}_2\text{N}]$ and the effects on power output were compared with the
181 performance of the terracotta separator in the absence of ionic liquid over the
182 ceramic surface (separator-1). Thus, $[\text{EMIM}][\text{Tf}_2\text{N}]$ was applied onto the inner
183 ceramic wall in contact with the catholyte. The ceramic materials were modified
184 by two methods resulting in two types of test to be investigated: (i) by uniformly
185 applying a layer of ionic liquid soaked in PTFE onto the whole of the inner wall
186 of the terracotta cylinder with a brush (separator-2) and (ii) by uniformly
187 applying a layer of ionic liquid but without PTFE (separator-3). In both cases,
188 the separators were left to dry overnight. All the configurations including ionic
189 liquid were prepared with a total amount of 1.5 g per cathode or separator. As
190 the amount of ionic liquid deposited is low compared with the high surface area
191 of the cathode chamber and some part is absorbed by the porous material, the
192 increase in separator thickness is negligible (approximately 200μ for the case
193 of separator-2 due to the inclusion of PTFE). There was a total of six set-ups for
194 investigating the performance of the ionic liquid $[\text{EMIM}][\text{Tf}_2\text{N}]$ in ceramic MFCs
195 (Table 1). It must be noted that the configurations named “cathode-1” and
196 “separator-1” are equivalent and served as the controls for the conditions

197 modified in the experiments. Three replicates of each type of MFC were built.
198 Fig. 2 shows a basic representation of the structure of the cathodes and the
199 separators researched.

200 [INSERT TABLE 1]

201 [INSERT FIGURE 2]

202 2.3. Data and analysis.

203 Voltage measurements (V) were recorded by ADC-24 Data Logger (Pico
204 Technology Cambridge shire, UK). The performance of the ceramic MFCs
205 assembled with different cathode and separator structures was analysed in
206 terms of power production. Polarisation and power curves were determined by
207 successively lowering the external resistive loads (R_L) from $\approx 1 \text{ M}\Omega$ to 11.78Ω ,
208 every 3 minutes, using an automatic load-controlled measurement tool [32]. Six
209 measurements were taken for each resistance at 30 second intervals. Current
210 and power output were calculated by $V = I \times R_L$ and $P = V^2/R_L$, respectively.
211 Internal resistance (R_{int}) of MFCs was calculated by $R_{int} = (OCV/I) - R_L$ applied
212 at the point of peak power, which is the point of maximum power transfer, where
213 OCV is the voltage in open-circuit conditions, I is the current under the external
214 load resistor and R_L is the external load resistor [33].

215 Measurements of pH and conductivity of each MFC were performed during the
216 experiments with a Hanna-8424 pH-meter (Hanna Instrument, UK) and 470-
217 Jenway conductivity meter (Camlab, UK), respectively.

218

219 3. Results and Discussion

220 *3.1. Carbon veil vs. carbon cloth*

221 As a preliminary study, the performance of two types of carbon materials,
222 carbon veil (cathode-1) and carbon cloth (cathode-2), were tested as diffusion
223 layers in MFCs fed with full strength activated sludge supplemented with
224 acetate (20 mM). Figure 3 depicts the polarisation and power curves with
225 standard error mean bars shown for the three replicates of each type of
226 cathode. The results from the triplicate tests, clearly show that the MFCs
227 working with carbon veil reached higher power levels than those with carbon
228 cloth. The maximum power and current values achieved by carbon veil
229 cathodes were 274.07 μW and 1154.88 μA , respectively, which were on
230 average more than double than those obtained with carbon cloth cathodes,
231 135.69 μW at 509.96 μA . Although the average value of OCV for the carbon
232 cloth (541 mV) was higher compared with that obtained with carbon veil (498
233 mV), the faster rate of change (steeper slope) suggests higher ohmic
234 resistance, which leads to a faster decrease in cell voltage. In fact, internal
235 resistance (R_{int}) in the case of carbon cloth-based MFCs, 539.1 Ω (calculated
236 according to the method described in section 2.3) is more than double the value
237 of R_{int} for the case of carbon veil-based MFCs, 225.5 Ω . The improved
238 performance of the carbon veil is strengthened by its lower cost, compared to
239 the carbon cloth [14]. These results were achieved with a total cathode area of
240 90 cm^2 in both cases. Although the carbon density is much higher for carbon
241 cloth, 120 $\text{g}\cdot\text{m}^{-2}$ with a thickness of 0.5 mm vs. 20 $\text{g}\cdot\text{m}^{-2}$ and 0.19 mm thickness
242 for carbon veil, the oxygen-permeability of carbon cloth is actually lower
243 according to the air permeability (section 2.2). The added advantage of carbon
244 veil is improved material integrity with minimal additional weight and thickness.

245 Consequently, carbon veil was selected as supporting and diffusion material for
246 the preparation of the cathodes when studying the influence of ionic liquids in
247 the subsequent experimental steps.

248

249 [INSERT FIGURE 3]

250

251 3.2. *Cathodes modified with ionic liquid.*

252

253 The voltage response of the MFCs using different cathode configurations
254 (cathode-1, cathode-3 and cathode-4) is shown in Fig. 4A. After the anode
255 maturing period with the cathode-1 in all MFCs, this type of cathode was
256 removed and replaced by the cathode types 3 and 4 in the appropriate
257 replicates. All anode compartments were emptied and replenished with 160 ml
258 of wastewater diluted 1:10 in deionised water and supplemented with acetate
259 with a final concentration of 20 mM. Fig. 4A shows the temporal voltage
260 response after the anolyte replenishment. For the sake of simplicity, the bar
261 errors for the replicates are not shown in Figure 4A, which is solely intended to
262 offer the voltage trends. Standard error mean values are however shown in
263 Figure 4B, which depicts the power levels achieved by each type of cathode.

264 The voltage response of the cells shows that the group of MFCs stabilises at
265 approximately 103, 129 and 167 mV for cathode-1, cathode-3 and cathode-4,
266 respectively, after 3 days (4305 min, without considering the anode maturing
267 period). The trend of maximum power follows the same order as the voltage
268 response, $P_{\max \text{ cathode-4}} > P_{\max \text{ cathode-3}} \gg P_{\max \text{ cathode-1}}$. These results suggest that
269 the MFCs using the ionic liquid 1-ethyl-3-methylimidazolium

270 bis(trifluoromethylsulfonyl)imide, [EMIM][Tf₂N] were significantly improved in
271 terms of power performance. MFC replicates using cathode-4, with the ionic
272 liquid as part of the mixture of the activated layer, reached a maximum power of
273 428.65 μ W at a current of 2238.51 μ A; the corresponding power and current
274 levels for the control replicates were 229.78 μ W at 1016.22 μ A. This shows that
275 the inclusion of the ionic liquid almost doubles the level of power and current
276 produced (an increase of up to 86.5%). When the ionic liquid was uniformly
277 spread over the activated carbon layer soaked in PTFE (cathode-3), the
278 performance of the MFCs also improved with values of 314.87 μ W and 1668.04
279 μ A of maximum power and current, respectively (Fig.4B), which represents an
280 increase of \approx 37 % over the maximum power obtained in the absence of ionic
281 liquid (cathode-1).

282

283 **[INSERT FIGURE 4]**

284

285 As seen in Figure 4, the effect of the ionic liquid used as part of the cathode is
286 visible for both cases when it is included in the mixture that forms the activated
287 carbon deposited on the carbon veil layer (cathode-4) and as a PTFE-soaked
288 layer over the carbon activated mixture once deposited on the electrode
289 (cathode-3). However as shown above, the level of power generated by MFCs
290 using the first configuration is higher. Although Figure 4 shows that MFCs using
291 Cathode-1 reached the highest OCV (476 mV), there is a rapid decrease of
292 voltage as current increases, whilst for the case of cathode-3 and cathode-4,
293 the slope for ohmic resistance is less steep, resulting in higher current and
294 power output and indicating improvement due to the addition of IL. As shown in

295 Table 2, the estimated values of R_{int} are higher for the MFCs working with
296 cathode-1 (245.9 Ω) compared with cathode-3 (119.6 Ω) and cathode-4
297 modifications (85.6 Ω). MFCs and fuel cells in general are subject to internal
298 losses such as activation, ohmic and mass-transfer over-potentials. The ohmic
299 losses in an MFC include both the electrode resistance to the flow of electrons,
300 and the cation-exchange-separator resistance to the flow of ions within the
301 anode and cathode electrolytes if present [34]. Through the application of the
302 ionic liquid in ceramic MFCs is expected to boost the ion transport from the
303 anode to the cathode through the ceramic separator [3], significantly improving
304 the level of power generated. The hydrophobic nature of the ionic liquid
305 [EMIM][Tf₂N] also allows the stability of the cathode performance [28].

306 Focusing on the comparison between cathode-3 and cathode-4, the way of
307 incorporating the ionic liquid described for cathode-3 implies the inclusion of an
308 additional layer of PTFE between the separator and the activated mixture itself.
309 It has been previously reported that the presence of an appropriate amount of
310 PTFE inside an activated carbon mixture for cathode construction results in a
311 more porous and highly textured mix, compared with a solely AC-based
312 cathode, enhancing oxygen diffusion and ion exchange [20]. However, cathode-
313 3 configuration also implies the superficial addition of PTFE (to soak the ionic
314 liquid) covering the surface of the catalyst that may improve the contact
315 between the separator and the carbon cathode, but also can lead to a reduction
316 of the cathode active area and thus the deterioration of the MFC performance
317 [35]. This may explain why the cathode-4, with the ionic liquid integrated in the
318 activated layer and not involving the addition of an extra PTFE layer,

319 outperforms the rest of the cathode configurations, as supported by the data of
320 maximum power and internal resistance provided above.

321

322 *3.3 Ceramic separator modified with ionic liquid.*

323

324 Several recent reports focused on the study of ionic liquids as electrolyte in
325 ionic exchange membranes for their application in MFCs [36]. The use of the
326 ionic liquid acting as an electrolyte was also included in this study through as
327 part of the separator by modifying the inner wall of the caves in two ways, (1) as
328 a layer of IL and PTFE directly applied on the ceramic material (separator-2)
329 and (2) as a layer of IL only (separator-3). As described in the previous section,
330 polarisation measurements were taken after establishing a stable voltage
331 response, once the MFCs were refilled with 160 ml of anolyte (described in
332 Materials and Methods). Figure 5 shows the power curves of the MFCs
333 incorporating these modifications, compared with those obtained with the
334 control set (separator-1). In this case, no improvement in the efficiency of the
335 MFCs working with a layer of PTFE-mixed IL spread over the inner ceramic wall
336 (separator-2) is observed or the level of power is severely limited when only the
337 IL is applied in the absence of PTFE (separator-3).

338

339 It must be noted that, for both types of modification i.e. separator-2 and
340 separator-3, the polarisation curves exhibit an irregular behaviour in the sector
341 after reaching the maximum power. This phenomenon has been previously
342 explored and described as overshoot due to the simultaneous decrease in
343 power and current, and has been associated with the underperformance of the

344 MFCs [30]. The overshoot phenomenon was not observable in the power
345 curves of the control set, even when the performance of these MFCs could be
346 improved by incorporating ionic liquid as part of the electrode. Therefore, the
347 occurrence of overshoot is not directly associated with the presence of a limiting
348 element such a low conductivity catholyte, but possibly with the presence of an
349 inhibiting component in the system. The overshoot phenomenon can be
350 attributed to the presence of the ionic liquid directly applied onto the ceramic
351 wall. But still, the MFCs replicates working with the separator-2, in presence of
352 PTFE, offer levels of power closer to those given by the control set (209.04 μW
353 vs. 229.78 μW).

354 When calculating the values of R_{int} of the MFCs using the different separator
355 configurations, it was found a significant increase in R_{int} for separator-3 (473.1
356 Ω) compared with that of separator-1 (245.9 Ω), and it was also higher for
357 separator-2 (288.6 Ω). In the case of separator-3, the lower regression
358 coefficient is due to the lack of stability of the MFC systems due to the
359 overshoot phenomenon. The ion exchange capacity of the ceramic material is
360 due to its hydrophilic nature and high cation exchange capacity [13]. When the
361 ionic liquid in the absence of PTFE is applied to the ceramic wall and is let to
362 dry, a certain amount of the catholyte is absorbed by the ceramic material,
363 penetrating the pores on the inner wall of the terracotta cylinder. Since the
364 performance of this type of MFCs lies on the transport of ions from the anode to
365 the cathode through the ceramic separator, the effects of depositing the ionic
366 liquid directly onto the separator can be observed in the values of internal
367 resistance and power output [37]. If the ionic is deposited on the ceramic wall
368 soaked with PTFE forming a mixture to fix the ionic liquid on the surface of the

369 ceramic wall, the blocking effect may be relieved compared to separator-2,
370 although internal resistance is still affected compared to separator-1 and no
371 improvement in power performance is observed. These results indicate that it is
372 not possible to improve the MFC performance in terms of power output by
373 integrating the electrolyte in the ceramic separator of the system by the
374 methods here described.

375

376 **[INSERT FIGURE 5]**

377

378 *3.4. Influence of the substrate concentration.*

379

380 In order to study the influence of the concentration of the substrate on the
381 power output and compare it with the effect of the ionic liquid, the MFCs
382 working with cathode-3 and cathode-4 and the control set were run at two
383 values of acetate concentration (20 and 100 mM), shown in Figure 6B. Voltage
384 and power values for the concentration of 20 mM correspond to the value given
385 in section 3.2. Figure 6C and D show the power and polarisation measurement
386 for the cathodes modified with ionic liquid (cathode-3 and cathode-4), including
387 the results for the MFCs working with the ionic liquid-free cathode at 100 mM as
388 control. The increase in the power output due to the addition of acetate is 26.1
389 % on average for the replicates using the cathode-1 (see Fig. 6.B), whilst the
390 increase due to the use of the ionic liquid is over 86% for the best case (see
391 Fig. 6.D). The comparison between the power curves of the replicates at 100
392 mM shows that the trend of maximum power levels at such concentration is the
393 same as is at 20 mM, $P_{\max \text{ cathode-4}} > P_{\max \text{ cathode-3}} \gg P_{\max \text{ cathode-1}}$ (see Table 2).

394 Regarding the replicates with ionic liquid, the higher percentage of increase in
395 power level is observed for cathode-3, with cathode-4 outperforming all the
396 other designs. These results also suggest that the cathode performance can be
397 one of the limiting factors in this type of MFCs in terms of power production,
398 since even the maximum power value achieved by the MFCs in the absence of
399 ionic liquid (cathode-1) at 100 mM (acetate), 289.73 μW , is almost half the best
400 result obtained with the ionic liquid present in the activated layer (cathode-4) at
401 20 mM, 428.65 μW (see Table 2). Moreover, although Figures 6.C and 6.D
402 show a higher value of OCV for cathode-1 (454 mV) compared to both cathode-
403 3 (376 mV at 20 mM and 414 mV at 100 mM) and cathode-4 (373 mV at 20 mM
404 and 404 mV at 100 mM), the differences observed in the slopes of the
405 polarization curves indicate a faster decrease in voltage, as current increases
406 for cathode-1. This results in an increase of the internal resistance (see Table
407 2), which remains much lower for cathode-4 and cathode-3 for both 20 and 100
408 mM.

409

410

[INSERT FIGURE 6]

411

412

[INSERT TABLE 2]

413

414 *3.5. Catholyte production.*

415

416 The operation of the MFC design used for this research implies the generation
417 of a certain amount of catholyte as a consequence of the transport of ion
418 species and water from the anode chamber through the ceramic wall. The

419 catholyte generated in the MFCs was of a transparent appearance. This type of
420 cylindrical ceramic-based MFC allows the production of catholyte of high salt
421 concentration whilst the recovery of clean water from the anode takes places by
422 electro-osmosis [37]. Figure 7 shows the amount of catholyte generated, pH
423 and conductivity after ≈ 5400 min. of operation by the main MFC configurations
424 studied, for the 20 mM acetate concentration case. As can be seen, there are
425 significant differences in the volume of catholyte generated, and it can be
426 assumed that the amount of catholyte generated directly depends on the level
427 of MFC performance as a consequence of the ion exchange through the
428 separator. These differences are not visible in the measurements of pH and
429 conductivity, which remained within the range of 10.6-12.1 for pH and 10.1-11.2
430 $\text{mS}\cdot\text{cm}^{-1}$ for conductivity, although the values of pH are slightly higher for the
431 catholyte samples generated by the cathode-3 and cathode-4.

432

[INSERT FIGURE 7]

433

434 **4. Conclusions**

435

436 The present work has investigated the application of ionic liquids in ceramic-
437 based MFCs in order to improve the level of power generation. For this
438 purpose, activated-carbon cathodes and terracotta separators were modified
439 with $[\text{EMIM}][\text{Tf}_2\text{N}]$ in pure form or soaked with PTFE. The results prove that with
440 the inclusion of the ionic liquid as part of the cathode a significant increase of
441 over 86% in power output is achieved. Amongst the methods tested, the mixture
442 of a certain amount of ionic liquid, activated carbon and PTFE forming one layer
443 pressed onto the diffusion layer (carbon veil) has shown to be the best option,

444 whilst the modification of the ceramic wall with [EMIM][Tf₂N] leads to the
445 deterioration of MFC performance. These results also hold true for a higher
446 concentration of the substrate. The MFCs using IL in the optimal way also
447 generated higher volumes of catholyte. Given the wide range of ionic liquids
448 available, further research may be needed to find the most appropriate ILs to be
449 applied in ceramic MFCs and optimise their use in this technology. In this
450 context, protic ionic liquids are of special interest in the field of MFCs, since the
451 ratio of proton conductivity to total ionic conductivity is an important parameter
452 in determining the performance of a fuel cell electrolyte. The study of the
453 transport of different ion species through the separator in the presence of ionic
454 liquid is another important factor from the point of view of the
455 characterization of the ceramic material, and hence future work is needed to
456 gain a better understanding of its performance, as well as how it may affect the
457 synthesised catholyte composition.

458

459 **ACKNOWLEDGEMENTS**

460 This work has been supported by the mobility grant awarded by Polytechnic
461 University of Cartagena ref. PMPDI-UPCT-2015. V.M. Ortiz-Martínez and M.J.
462 Salar-García thank the Ministry of Education and the Ministry of Economy and
463 Competitiveness for supporting their doctoral theses (Ref: FPU12/05444 and
464 BES-2012-055350, respectively). Ioannis Ieropoulos is supported by an EPSRC
465 New Directions award, grant no. EP/L002132/1.

466

467 **References**

468

469 [1] D. Pant, G. V. Bogaert, L. Diels, K. Vanbroekhoven. A review of the
470 substrates used in microbial fuel cells (MFCs) for sustainable energy
471 production. *Bioresour Technol*, 101 (2010) 1533-1543.

472 [2] H.M. Wang, Z.Y.J. Ren. A comprehensive review of microbial
473 electrochemical systems as a platform technology. *Biotechnol Adv*, 31 (2013)
474 1796-1807.

475 [3] Z. Ge, J. Li; L. Xiao, Y.R. Tong, Z. He. Recovery of Electrical Energy in
476 Microbial Fuel Cells. *Scienc & Technol Lett*, 1 (2014) 137-141.

477 [4] V.M. Ortiz-Martínez, M.J. Salar-García, A.P. de los Ríos, F.J. Hernández-
478 Fernández, J.A. Egea, L.J. Lozano. Developments in Microbial Fuel Cell
479 Modeling. *Chem Eng J*, 271 (2015) 50-60.

480 [5] I. Ieropoulos, J. Greenman, C. Melhuish. Improved energy output levels from
481 small-scale Microbial Fuel Cells. *Bioelectrochem*, 78 (2010) 44-50.

482 [6] H. Wang, J-D Park, Z. J. Ren. Practical Energy Harvesting for Microbial Fuel
483 Cells: A Review. *Environ Sci Technol*, 49 (2015) 3267–3277.

484 [7] R.A. Rozendal, H.V.M. Hamelers, C.J.N. Buisman. Effects of membrane
485 cation transport on pH and microbial fuel cell performance. *Environ Sci Technol*
486 40 (2006) 5206–5211

487 [8] W.-W. Li, G.-P. Sheng, X.-W. Liu, H.-Q. Yu. Recent advances in the
488 separators for microbial fuel cells. *Bioresour Technol*, 102 (2010) 244-252.

- 489 [9] J. Winfield, L. D. Chambers, J. Rossiter, John Greenman, I. Ieropoulos.
490 Urine-activated origami microbial fuel cells to signal proof of life. *J Mater Chem*
491 *A* 3 (2015) 7058-7065.
- 492 [10] Papaharalabos G., Greenman J., Melhuis C., Santoro C., d, P. Cristiani, B.
493 Li, I. Ieropoulos. Increased power output from micro porous layer (MPL)
494 cathode microbial fuel cells (MFC). *Int J of Hydrogen Energ*, 38 (2013) 11552-
495 11558.
- 496 [11] D. H. Park and J.G. Zeikus. Improved fuel cell and electrode designs for
497 producing electricity from microbial degradation. *Biotechnol Bioeng*. 81 (2003)
498 348-355.
- 499 [12] M. Behera, P.S. Jana, M.M. Ghangrekar. Performance evaluation of low
500 cost microbial fuel cell fabricated using earthen pot with biotic and abiotic
501 cathode. *Bioresour Technol* 101 (2010) 1183-1189.
- 502 [13] J. Winfield, J. Greenman, D. Huson, I. Ieropoulos. Comparing terracotta
503 and earthenware for multiple functionalities in microbial fuel cells. *Bioproc*
504 *Biosyst Eng*, 36 (2013) 1913-1921.
- 505 [14] I. Gajda, A. Stinchcombe, J. Greenman, C. Melhuish, I. Ieropoulos.
506 Ceramic MFCs with internal cathode producing sufficient power for practical
507 applications. *Int J Hydro Energ* (2015). (DOI: 10.1016/j.ijhydene.2015.06.039).
- 508 [15] M. Zhou, M. Chi, J. Luo, H. He and T. Jin. An overview of electrode
509 materials in microbial fuel cells. *J Power Sources*, 196 (1011) 4427–4435.
- 510 [16] C. Santoro, K. Artyushkova, S. Babanova, P. Atanassov, I. Ieropoulos, M.
511 Grattieri, et al., Parameters characterization and optimization of activated

512 carbon (AC) cathodes for microbial fuel cell application. *Bioresour Technol*
513 163C (2014) 54–63.

514 [17] S. Chen, Y. Chen, G. He, S. He, U. Schroeder, H. Hou. Stainless steel
515 mesh supported nitrogen-doped carbon nanofibers for binder-free cathode in
516 microbial fuel cells. *Biosens Bioelectron*, 34 (2012) 282–285.

517 [18] L. Feng, Y. Yan, Y. Chen, L. Wang. Nitrogen-doped carbon nanotubes as
518 efficient and durable metal-free cathodic catalysts for oxygen reduction in
519 microbial fuel cells. *Energy Environ Sci*, 4 (2011) 1892–1899.

520 [19] H. Dong, H. Yu, X. Wang, Q. Zhou, J. Feng. A novel structure of scalable
521 air-cathode without Nafion and Pt by rolling activated carbon and PTFE as
522 catalyst layer in microbial fuel cells. *Water Res*, 46 (2012) 5777–5787.

523 [20] R. Lin, T. Zhao, H. Zhang, C. Cao, B. Li, J. MA. Influence of PTFE on
524 Electrode Structure for Performance of PEMFC and 10-Cells Stack. *Chin J*
525 *Mech Eng*, 25 (2012) 1171-1175.

526 [21] K. Ghandi. A review of ionic liquids, their limits and applications. *Green and*
527 *Sustainable Chemistry*, 4 (2014) 44-53.

528 [22] D. Wei, A. Ivask. Applications of ionic liquids in electrochemical sensors.
529 *Analytica Chimica Acta*, 28 (2008) 126-135.

530 [23] M.C. Buzzeo, R.G. Evans, R.G. Compton. Non-haloaluminate room-
531 temperature ionic liquids in electrochemistry: a review. *Chem Phys Chem*, 5
532 (2004) 1106-1120.

533 [24] D.R. Macfarlane, N. Tachikawa, M. Forsyth, J.M. Pringle, P.C. Howlett, G.
534 D. Elliott, J.H. Davis, M. Watanabe, P. Simons, C.A. Angell. Energy applications
535 of ionic liquids. *Energy Environ Sci*, 7 (2014) 232-250.

536 [25] M. Armand, F. Endres, D.R. MacFarlane, H. Ohno, B. Scrosati. Ionic-liquid
537 materials for the electrochemical challenges of the future. *Nat Mater*, 8 (2009)
538 621-629.

539 [26] M. J. Salar-García, V. M. Ortiz-Martínez, A.P. de los Ríos, F.J. Hernández-
540 Fernández. A method based on impedance spectroscopy for predicting the
541 behavior of novel ionic liquid-polymer inclusion membranes in microbial fuel
542 cells. *Energy*, (2015) (doi: 10.1016/j.energy.2015.05.149).

543 [27] M. Galiński, A. Lewandowski and I. Stępnia. Ionic liquids as electrolytes.
544 *Electrochim Acta* 51 (2006) 5567–5580.

545 [28] W. Lu, L. Qu, K. Henry, L. Dai. High performance electrochemical
546 capacitors from aligned carbon nanotube electrodes and ionic liquid
547 electrolytes. *J Power Sources*, 189 (2009) 1270–1277.

548 [29] A. Lewandowski, A. Świdorska-Mocek. Ionic liquids as electrolytes for Li-
549 ion batteries-An overview of electrochemical studies. *J Power Sources* 194
550 (601-609).

551 [30] J. Winfield, I. Ieropoulos, J. Greenman, J. Dennis. The overshoot
552 phenomenon as a function of internal resistance in microbial fuel cells.
553 *Bioelectrochem*, 81 (2011) 22–27.

554 [31] C. Santoro, K. Artyushkova, I. Gajda, S. Babanova, A. Serova, P.
555 Atanassov, J. Greenman et al. Cathode materials for ceramic based microbial

556 fuel cells (MFCs). *Int. J. Hydrogen Energ*, (2015)
557 (doi:10.1016/j.ijhydene.2015.07.054).

558 [32] N. Degrenne, F. Buret, B. Allard, P. Bevilacqua. Electrical energy
559 generation from a large number of microbial fuel cells operating at maximum
560 power point electrical load. *J Power Sources*, 205 (2012) 188-193.

561 [33] I. Ieropoulos, J. Greenman, C. Melhuish, C. (2008). Microbial fuel cells
562 based on carbon veil electrodes: Stack configuration and scalability. *Int J Energ*
563 *Res*, 32 (2008) 1228–1240.

564 [34] B.E. Logan, B. Hamelers, R. Rozendal, U Schröder, J Keller, S. Freguia,
565 P. Aelterman, W. Verstraete, K. Rabaey. *Microbial Fuel Cells: Methodology and*
566 *Technology. Environm Sci Technol*, 40 (2006) 5181-5192.

567 [35] R. Lin, T. Zhao, H. Zhang, C. Cao, B. Li and J. Ma. Influence of PTFE on
568 electrode structure for performance of PEMFC and 10-cells stack. *Chin J Mech*
569 *Eng*, 25 (2012) 1171-1175.

570 [36] M. Díaz, A. Ortiz, I. Ortiz. Progress in the use of ionic liquids as electrolyte
571 membranes in fuel cells. *J Membrane Sci*, 469 (2014) 379–396.

572 [37] I. Gajda, J. Greenman, C. Melhuish, I. Ieropoulos. Simultaneous electricity
573 generation and microbially-assisted electrosynthesis in ceramic MFCs.
574 *Bioelectrochem*, 104 (2015) 58–64.

575

576

577

578 **Figure captions.**

579

580 **Fig. 1.** Ceramic MFC set-up.

581 **Fig. 2.** Configuration of the cathodes and the separators studied. IL is

582 represented by the positive and negative charges.

583 **Fig. 3.** Polarisation and power curves of the MFCs with carbon veil (cathode-1)

584 and carbon cloth (cathode-2).

585 **Fig. 4.** A) Voltage response of different MFCs cathode configurations. B)

586 Polarisation and power curves of MFCs working with cathode-1 (without ionic

587 liquid), cathode-3 (ionic liquid layer) and cathode-4 (ionic liquid mixture),

588 including SEM error bars for replicates.

589 **Fig. 5.** Polarisation and power curves of MFCs working with separator-1,

590 separator-2 and separator-3 configurations, including error bars for replicates.

591

592 **Fig. 6.** A) Voltage response of the different MFCs cathode configurations at 100

593 mM acetate concentration. B, C and D) Effect of the substrate concentration on

594 the power performance.

595

596 **Fig. 7.** Volume, pH and conductivity of the catholyte generated by the MFCs.

597

598

599

600

601

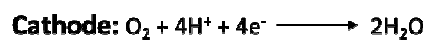
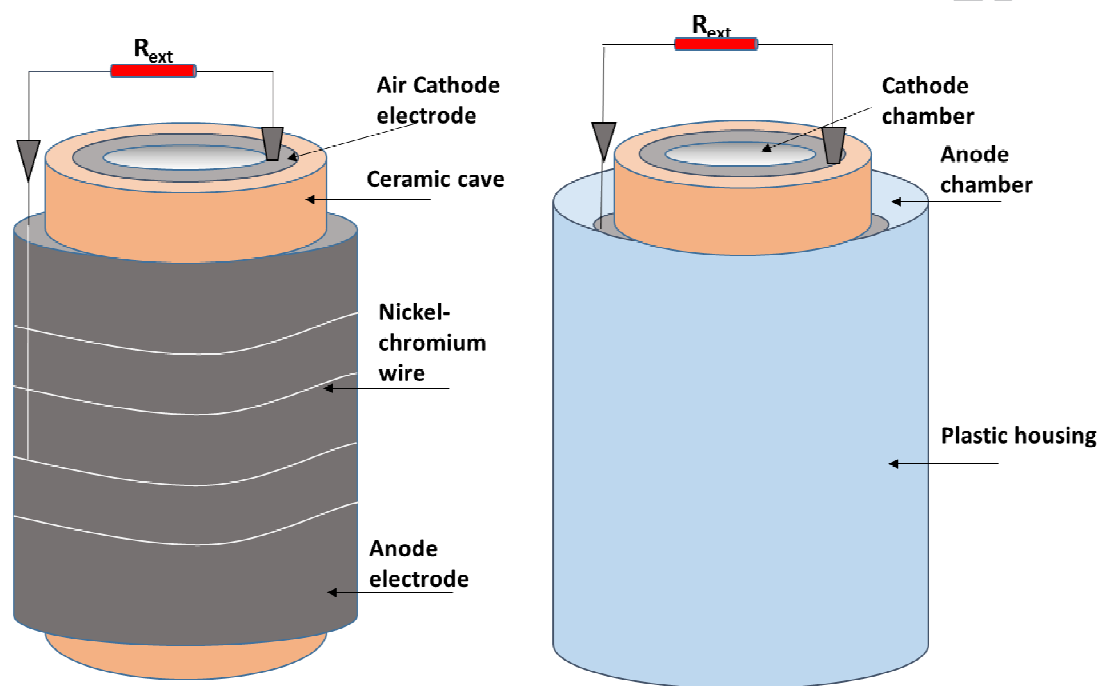
602

603

604

605 **Figures.**

606

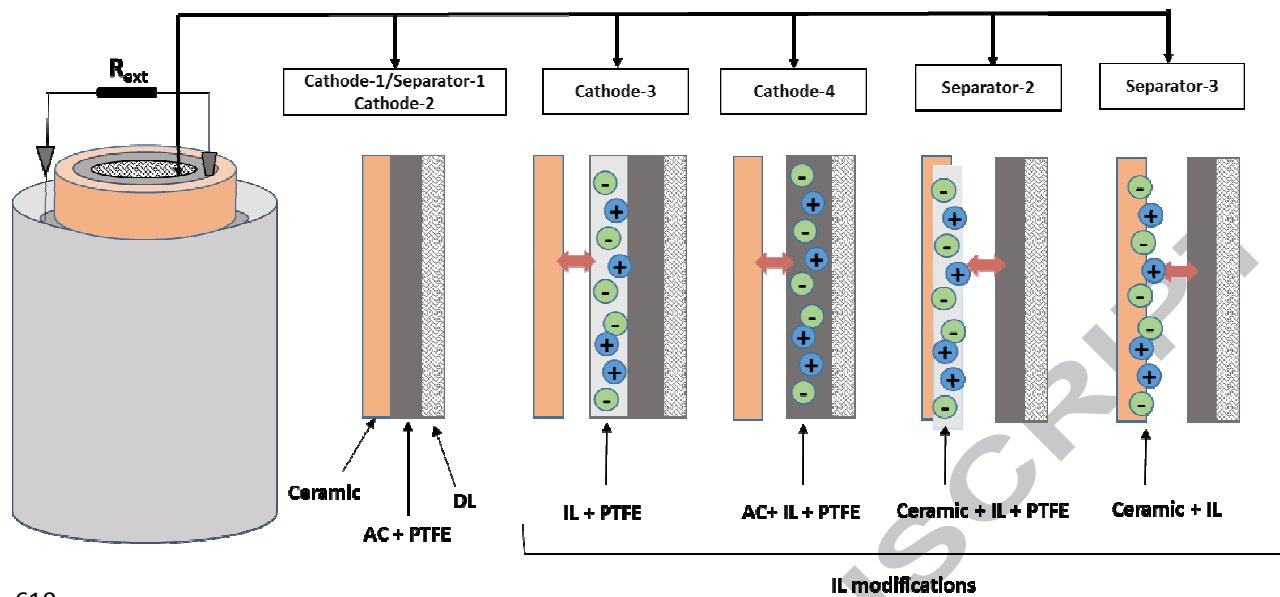


607

608

609 **Fig. 1**

609



610

611

612

613

614

615

616

617

618

619

Fig. 2.

ACCEPTED

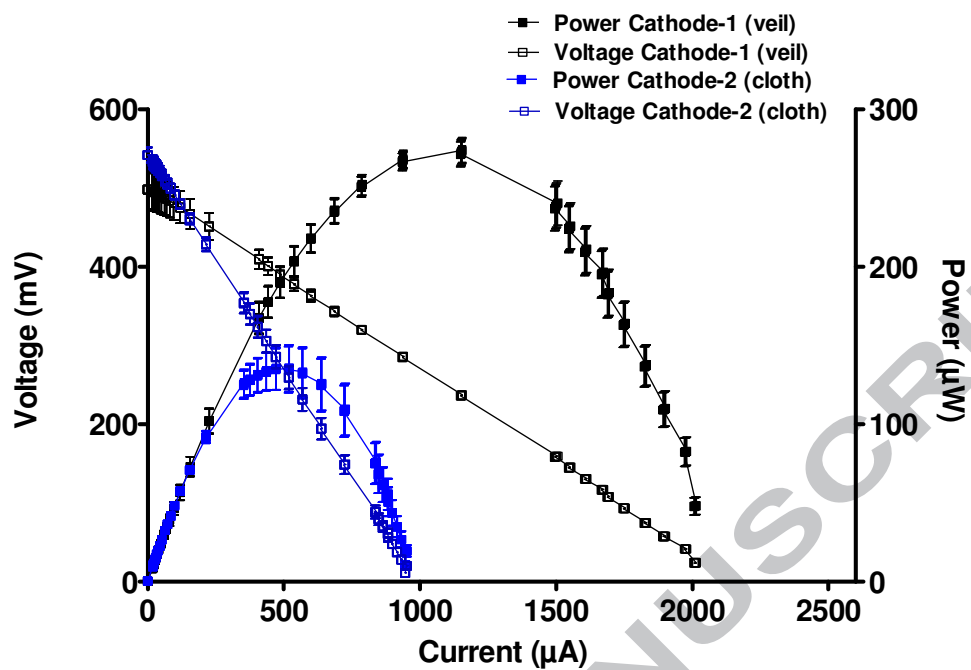


Fig. 3.

620

621

622

623

624

625

626

627

628

629

630

631

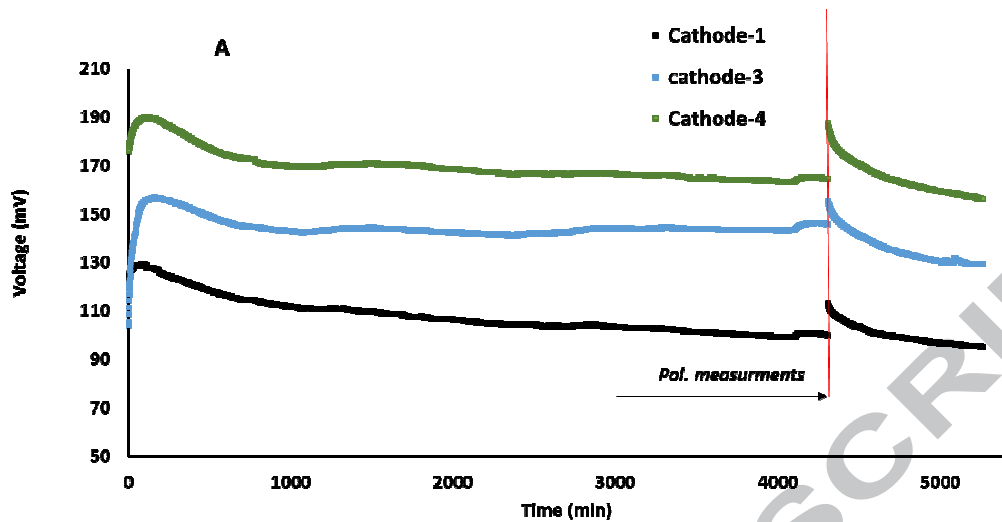
632

633

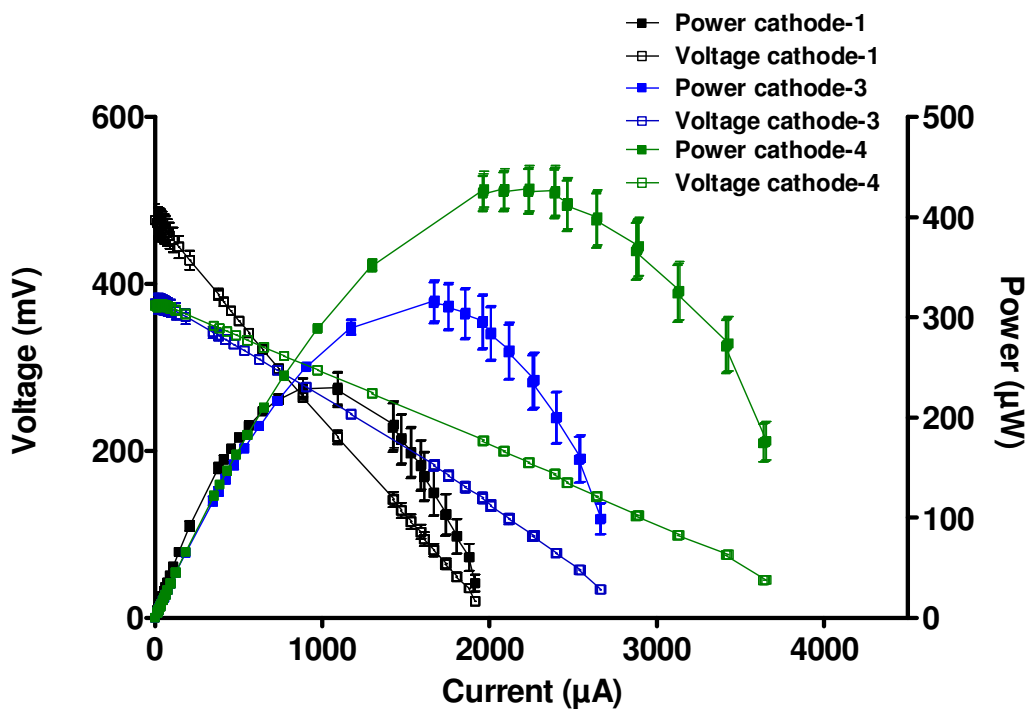
634

635

636



637



638

639

640

641

642

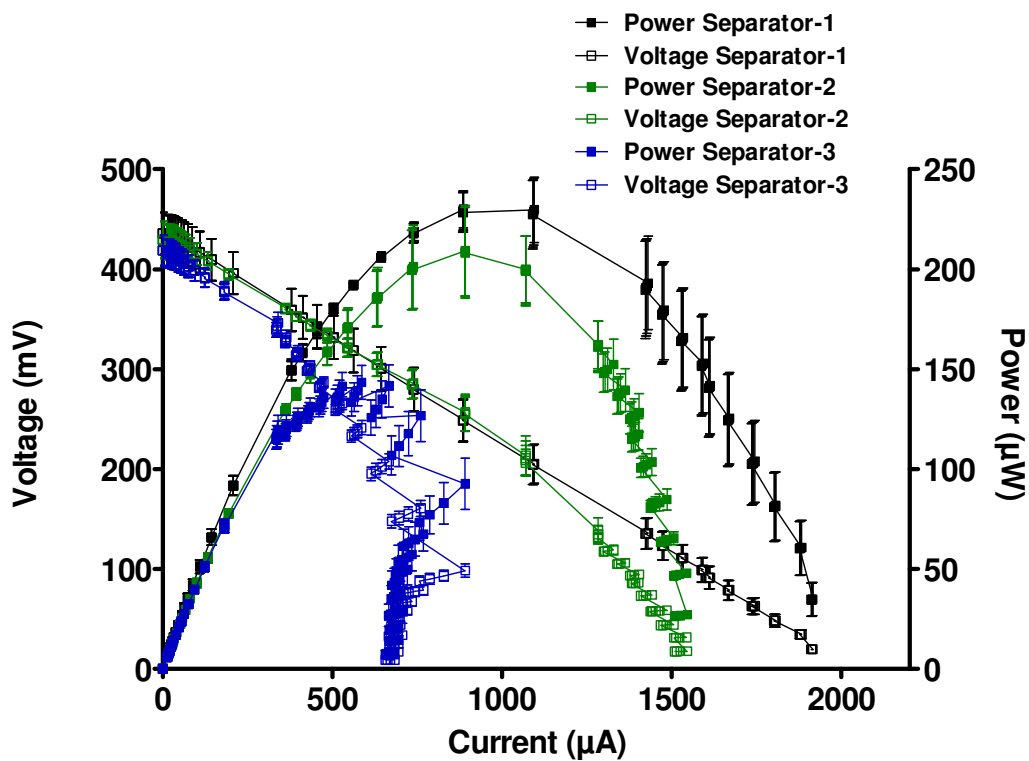
643

644

645

Fig. 4.

646



647

648

649

650

651

652

653

654

655

656

657

658

659

660

661

662

663

Fig. 5.

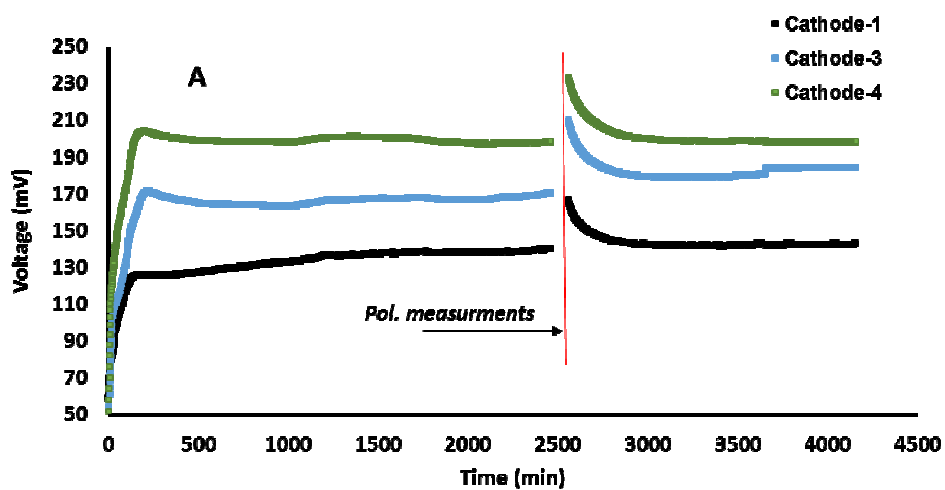
664

665

666

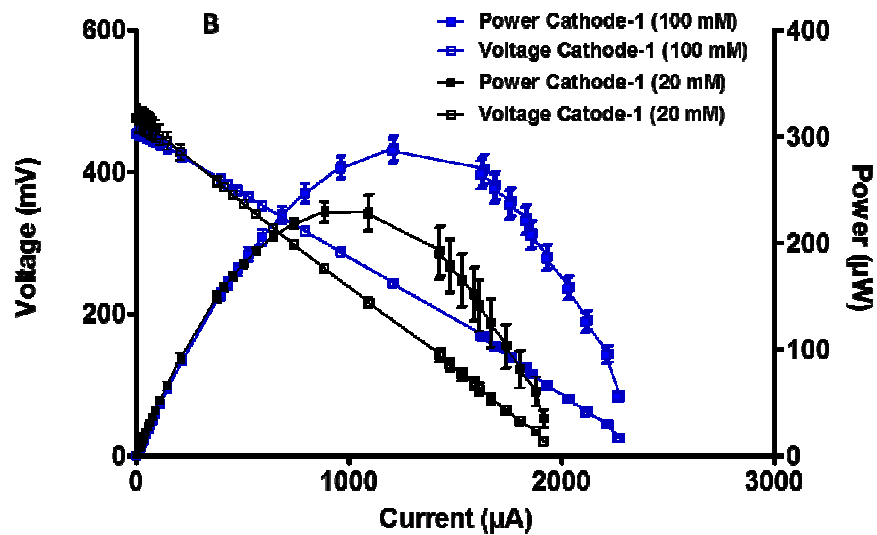
667

668



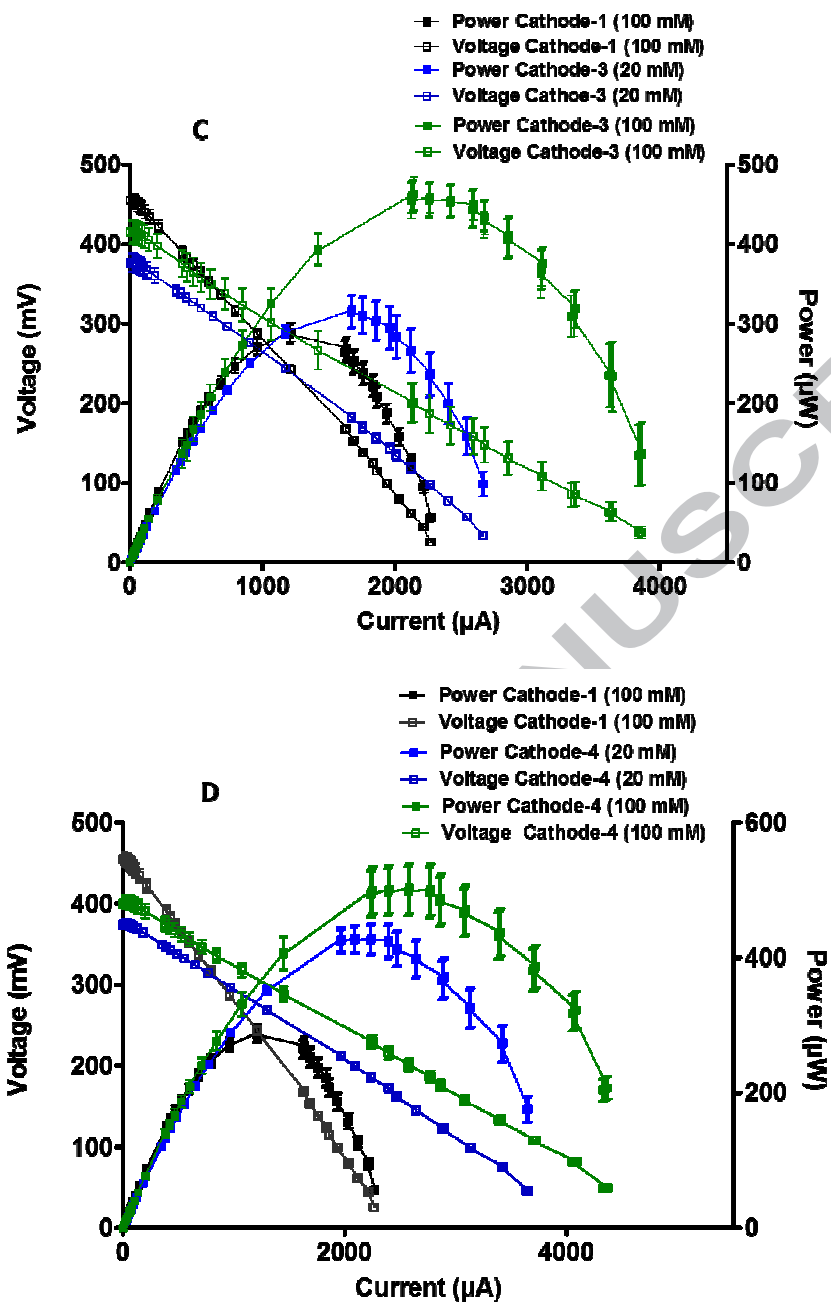
669

670



671

672



673

674

675

676

677

678

679

680

681

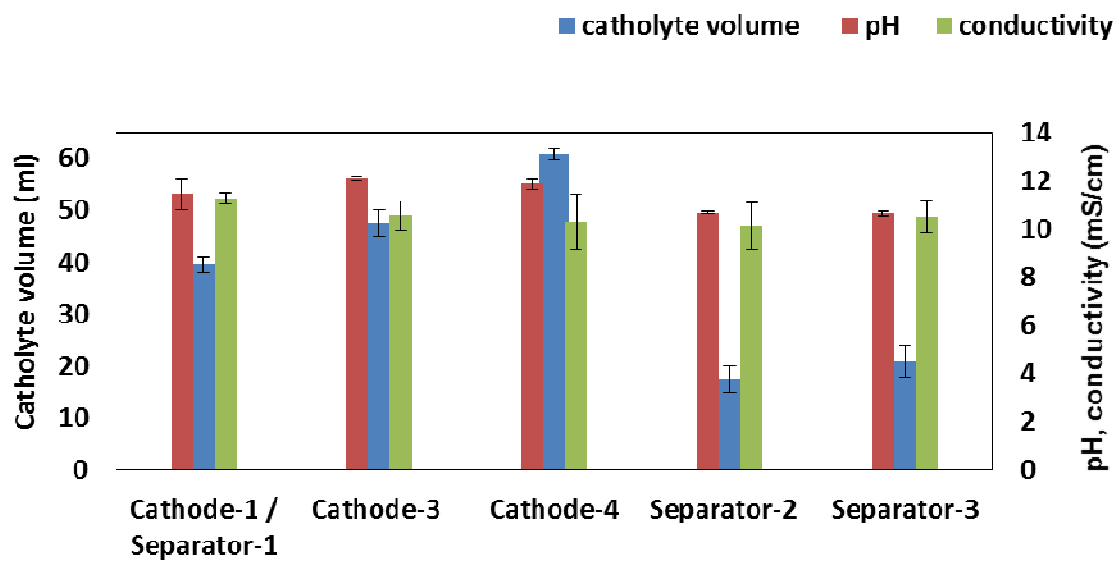
682

Fig. 6.

683

684

685



686

687

688

689

Fig. 7.

ACCEPTED

690 **Tables.**

691

692 **Table 1.** Six types of MFCs studied.693 **Table 2.** Maximum power output and associated electrical current.

694

MFC type	Diffusion Layer	Cathode	Inner Ceramic Wall
Cathode-1 / Separator-1	Carbon veil	AC + PTFE	Clean
Cathode-2	Carbon cloth	AC + PTFE	Clean
Cathode-3	Carbon veil	[AC + PTFE] _{Mixture} + [IL + PTFE] _{Layer}	Clean
Cathode-4	Carbon veil	[AC + PTFE + IL] _{Mixture}	Clean
Separator-2	Carbon veil	AC + PTFE	IL + PTFE
Separator-3	Carbon veil	AC + PTFE	IL

695

696

Table 1.

697

698

699

700

	20 mM acetate (1:10)			100 mM acetate (1:10)		
	P _{max} (μW)	I (mA)	R _{int} (Ω)	P _{max} (μW)	I (mA)	R _{int} (Ω)
Cathode-1	229.78	1016.22	245.9	289.73	1211.82	169.2
Cathode-3	314.87	1668.4	119.6	459.22	2229.93	93.5
Cathode-4	428.65	2238.51	85.6	502.92	2581.63	75.5

701

702

Table 2.

703

704

705 **Highlights**

706

- 707 ▪ **IL-modified cathodes improve the performance of ceramic MFCs.**
- 708 ▪ **[EMIM][Tf₂N]-based MFCs offer 86 % more power output compared**
- 709 **with IL-free MFCs.**
- 710 ▪ **Optimal performance of ILs as part of the activated layer of the**
- 711 **cathode.**

712

713